

# Improvement on Mechanical Property of B<sub>4</sub>C/Al Composites by Addition of Ti Through Interfacial Reaction

Ruan Qing<sup>1</sup>, Jia Yuzhen<sup>2</sup>, Zheng Jiyun<sup>2</sup>, Li Qiulin<sup>3</sup>, Liu Wei<sup>1</sup>, Shu Guogang<sup>4</sup>

<sup>1</sup> Tsinghua University, Beijing 100084, China; <sup>2</sup> Science and Technology on Reactor Fuel and Materials Laboratory, Nuclear Power Institute of China, Chengdu 610041, China; <sup>3</sup> Graduate School at Shenzhen, Tsinghua University, Shenzhen 518055, China; <sup>4</sup> China Nuclear Power Engineering Co. Ltd, Shenzhen 518055, China

**Abstract:** A fine bonded interface is essential for the property of metal matrix composites. A boron carbide reinforced aluminum composites (B<sub>4</sub>C/Al) was fabricated by liquid stirring technology. The effect of interfacial reaction on the microstructure and mechanical behavior of B<sub>4</sub>C/Al composites was explored by addition of Ti. The results show that through B<sub>4</sub>C-Al melt interfacial reaction, Ti element strongly enriches at the interface. A dense and continuous nanoscale layer of TiB<sub>2</sub> forms on the surface of B<sub>4</sub>C particles. Interfacial modification is achieved by interfacial reaction. Since the formed TiB<sub>2</sub> layer has good wettability and bonding, interfacial defects are eliminated. With the increasing of reaction degree, such as Ti content and reaction time, the strength of B<sub>4</sub>C/Al composites gradually improves. Severe interfacial reaction introduces lots of nano-scale TiB<sub>2</sub> crystals into the matrix, which as in situ second reinforcement also improves the strength of B<sub>4</sub>C/Al composites. Fracture behavior of B<sub>4</sub>C/Al composites with different interfacial modification was discussed at last.

**Key words:** B<sub>4</sub>C/Al composites; Ti; interfacial reaction; mechanical property

Due to the excellent neutron absorption ability of B<sup>10</sup> atom, B<sub>4</sub>C/Al composites have been widely applied in nuclear power industry for spent fuels transportation and storage in recent years<sup>[1-3]</sup>. Since it is more flexible and cost-saving than the wet storage, dry storage technology attracts more and more interest. To obtain larger storage volume, B<sub>4</sub>C/Al composites are expected to be both functional and structural neutron absorber materials. However, in the service environment of dry storage technology, B<sub>4</sub>C/Al composites are subjected to elevated temperature between 300~400 °C for long time, in addition to high level of gamma and neutron radiation<sup>[4]</sup>. These severe conditions have highlighted the demand for mechanical property of B<sub>4</sub>C/Al composites.

Interfacial bonding state is important for the mechanical behavior of particle reinforced metal matrix composites (MMCs)<sup>[5,6]</sup>. Under an applied load, the load is transferred from the weaker matrix, across the matrix-reinforcement interface, to the typically higher stiffness reinforcement. A

strong interface will usually allow effective load transfer from the matrix to reinforcement, leading to improved strength, stiffness and resistance to environmental attack<sup>[7]</sup>. Zhang et al<sup>[8]</sup> investigated the effect of interface damage on constitutive behavior of B<sub>4</sub>C/Al composites and found that imperfect interface microstructure resulted in decreased flow strength and the failure strain. Weak interface bonding led to interfacial debonding dominated fracture behavior<sup>[9]</sup>. Tham et al<sup>[10,11]</sup> prepared SiC/Al composites with two distinct interfacial microstructures by melt technology. The formation of a thin Al<sub>4</sub>C<sub>3</sub> reaction layer along SiC-Al interface helped to overall improve material's mechanical properties like tensile strengths and work-hardening rate. The Al<sub>4</sub>C<sub>3</sub> layer changed the fracture pattern from one involving interfacial decohesion to one where particle breakage was dominant.

When B<sub>4</sub>C/Al composites are produced by molten metal technology, the reaction between B<sub>4</sub>C and Al melt has to be seriously considered<sup>[12]</sup>. A common interfacial reaction

Received date: June 19, 2018

Foundation item: Key Project of Shenzhen Science and Technology Innovation Committee (2013966003)

Corresponding author: Zheng Jiyun, Master, Science and Technology on Reactor Fuel and Materials Laboratory, Nuclear Power Institute of China, Chengdu 610041, P. R. China, Tel: 0086-28-85906082, E-mail: zhengjiyun@aliyun.com

Copyright © 2019, Northwest Institute for Nonferrous Metal Research. Published by Science Press. All rights reserved.

occurred during melt stirring period, as shown in expression (1)<sup>[13,14]</sup>:



Since this reaction is much severe to produce many second particles  $\text{AlB}_2$ , the fluidity of  $\text{Al-B}_4\text{C}$  melt rapidly decreased in a short time, which brings difficulty in the casting process. In order to suppress above reaction, Ti element is added into the melt. Then reaction is changed to be expression (2)<sup>[15-17]</sup>:



$\text{AlB}_2$  particles are replaced by  $\text{TiB}_2$  layer, which tightly surrounds on the surface of  $\text{B}_4\text{C}$  particles, reducing the rate of  $\text{B}_4\text{C}$  degradation as a protective layer. Fluidity can be maintained for long time. Although it is realized that addition of Ti has an influence on  $\text{B}_4\text{C-Al}$  interface, the effect of Ti was mainly studied for the preparation process in last decade. According to our previous research<sup>[15]</sup>, the thickness of  $\text{TiB}_2$  layer can be less than 1  $\mu\text{m}$ , even tens of nanometers. It is believed that interfacial reaction layers with nano-level thickness are beneficial for mechanical property since they usually enhance both chemical and mechanical bonding between the particle and matrix<sup>[18,19]</sup>. Luo<sup>[20]</sup> indicated that chemical interface with coherency or semicoherency bonding improves load transfer and hence favors good mechanical property. However, the inner relationship between interfacial reaction and mechanical behavior of  $\text{B}_4\text{C/Al}$  composites is not clear.

In this paper, the effect of interfacial reaction on mechanical property of  $\text{B}_4\text{C/Al}$  composites with addition of Ti element was investigated under an objective of improving mechanical behavior. It is expected to obtain proper extent of interfacial reaction and optimal interfacial microstructure for  $\text{B}_4\text{C/Al}$  composites. Thus, as neutron absorber materials,  $\text{B}_4\text{C/Al}$  composites with fine combination of mechanical property and neutron shielding ability could satisfy the requirement of dry storage and transportation application of spent fuels.

## 1 Experiment

Four batches of  $\text{B}_4\text{C/Al}$  billets were prepared by varying Ti content and stirring time. Preparation parameters are shown in Table 1. The processing procedure of stirring-casting method was as follows: commercially pure Al and Al-Ti master alloy were first melted in a furnace under vacuum condition ( $<10$  Pa). The temperature was kept at 730  $^\circ\text{C}$  after long time holding.  $\text{B}_4\text{C}$  powders with average diameter  $D=24.937$   $\mu\text{m}$  and span of size distribution  $\lambda=1.34$  were added into the melt. Masses of all materials were designed for  $\text{B}_4\text{C/Al}$  composites consisting of 15 wt%  $\text{B}_4\text{C}$  and corresponding Ti content. In the following part, IDs: C0.5, C1, C1.5 and C2.5 are used to represent four composites with Ti content of 0.5, 1, 1.5 and 2.5 (in wt%), respectively. A mechanical stirrer was used to incorporate  $\text{B}_4\text{C}$  particles through agitating the melt. Stirring speed was constant at 500 r/min. Once stirring time was reached, the melt was directly cast into a preheated rectangle mould at 420  $^\circ\text{C}$ . The whole casting process was under

**Table 1 Preparation parameters of  $\text{B}_4\text{C/Al}$  composite**

Serial number of billets	1	2	3	4
Ti content/wt%	0.5	1	1.5	2.5
Stirring time/min	10	10	10	55
IDs	C0.5	C1	C1.5	C2.5

protective atmosphere of argon. To eliminate casting defects,  $\text{B}_4\text{C/Al}$  billets with size of 20 mm  $\times$  30 mm  $\times$  50 mm were hot rolled at 450  $^\circ\text{C}$  to a final sheet with thickness of 1 mm. Subsequently  $\text{B}_4\text{C/Al}$  composites sheets were annealed at 380  $^\circ\text{C}$  for 2 h.

Mechanical and ion beam (IB-09020CP, JEOL) polishing methods were used to process samples. Scanning electron microscopy (SEM, TESCAN MIRA 3 LMH), equipped with energy dispersive spectrometer (EDS) and electron back-scattered diffraction (EBSD), was used to characterize the microstructure of interface and matrix. To identify reaction phases, X-ray diffraction test (Rigaku Rint 2200, Tokyo, Japan) was performed on solid and powder samples, which were obtained by dissolving solid samples in HCl distilled water solution (1.2 mol/L) to decrease the diffraction of Al matrix. Tensile tests with an extensometer were performed at room temperature using a universal tensile machine in accord to ISO 6892-1: 2009. The moving speed was constant at 0.5 mm/min during the whole test. Fig.1 shows the size of tensile specimens. Then the fracture surface of failed tensile specimens was observed by SEM.

## 2 Results and Discussion

### 2.1 Microstructure characterization

Fig.2 presents the  $\text{B}_4\text{C}$  particles distribution and EBSD images of  $\text{B}_4\text{C/Al}$  composites with different preparation conditions. Nearly uniform distribution of  $\text{B}_4\text{C}$  particles is obtained in all aluminum matrix, although some minor difference exists. It can be assumed that the distribution of  $\text{B}_4\text{C}$  particles in all composites is similar and the influence of  $\text{B}_4\text{C}$  particle distribution on mechanical property could be ignored in following discussion. The microstructure of matrix also indicates that prepared composites are fully dense. In order to eliminate deformation structure after hot rolling, all sheets were annealed at 380  $^\circ\text{C}$  for 2 h. As shown in Fig.2e~2h, the grains of all  $\text{B}_4\text{C/Al}$  composites transform to equiaxial grains during crystallization process.  $\text{B}_4\text{C}$  particles are mainly located at the boundary of aluminum crystals. Normalized matrix microstructure will be beneficial to individually

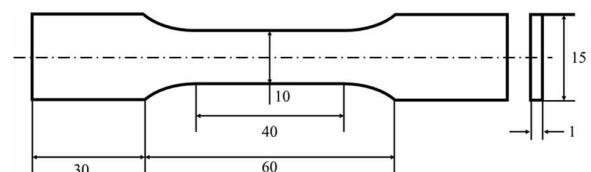


Fig.1 Size of tensile specimen

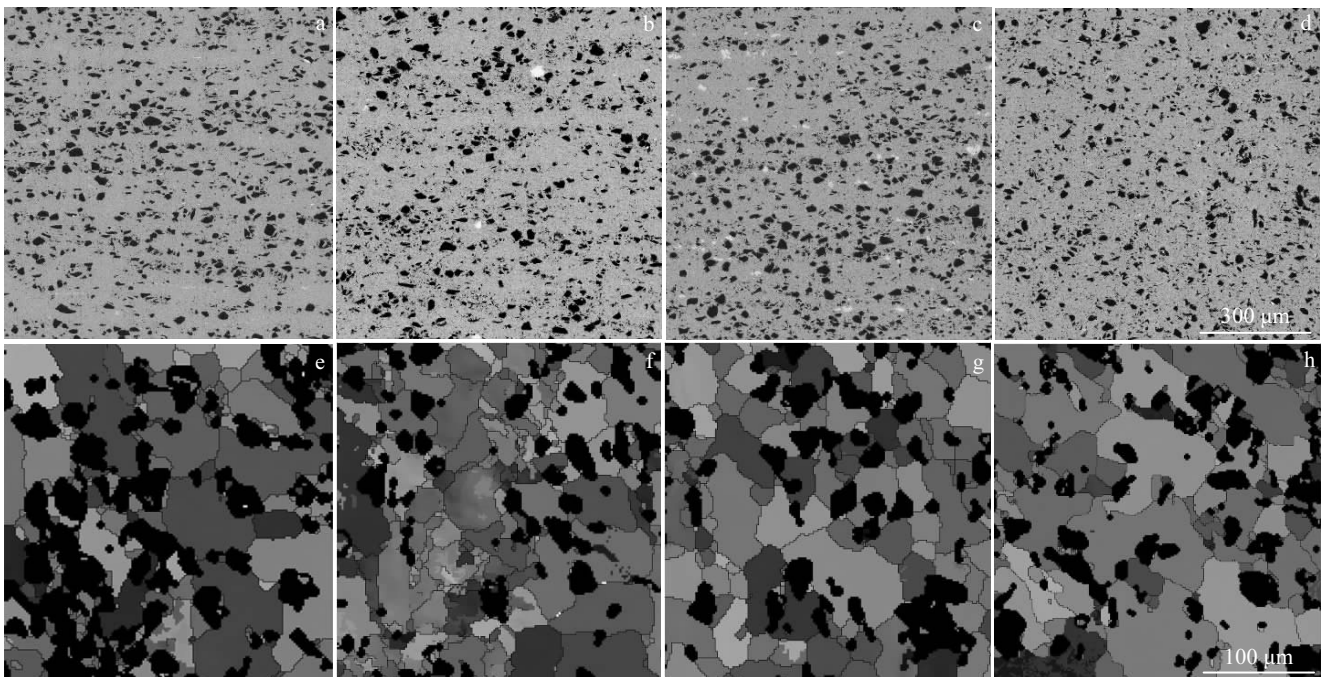


Fig.2 Particles distribution (a~d) and EBSD images (e~h) of annealed  $B_4C/Al$  composites: (a, e) C0.5, (b, f) C1, (c, g) C1.5, and (d, h) C2.5 (the black and white particles are  $B_4C$  and  $Al_3Ti$ , respectively)

discuss the effect of interface microstructure on mechanical property of  $B_4C/Al$  composites.

Phase identification results of  $B_4C/Al$  composites are shown in Fig.3. It is obvious that the phases in  $B_4C/Al$  composites are complex, basically concluding  $B_4C$ , Al and  $TiB_2$ . However,  $Al_3Ti$ , a binary equilibrium phase in Al-Ti alloy, is detected in C1.5, which indicates excess Ti element in the matrix, as the white particles shown in Fig.2c. Besides,  $Al_3BC$  is detected in C2.5 sample with long reaction time, indicating a severe reaction process through Eq.(2). The formation of  $TiB_2$  illustrates that a strong reaction occurs in the Al- $B_4C$ -Ti system which features for transformation of Ti element from  $Al_3Ti$  to  $TiB_2$ . Fig.4 shows the distribution of Ti element in prepared  $B_4C/Al$  composites. Ti element obviously enriches on the surface of  $B_4C$  particles. The enrichment of Ti element at the Al- $B_4C$  interface is achieved through Eq.(2)<sup>[15]</sup>, which features for precipitation of  $TiB_2$  on  $B_4C$  surface. However, difference exists in the abundance degree of Ti element. In the matrix of C0.5, Ti enrichment layer is not continuous. Some  $B_4C$  particles' surface is even lack of reaction product  $TiB_2$ . With the increase of Ti content,  $TiB_2$  layer becomes more continuous and compact. As for the C2.5, Ti atoms are not only completely coated on the surface of  $B_4C$  particles, but also gather in the aluminum matrix, as shown in Fig.4d and 4h. Besides, the size of  $TiB_2$  crystals in matrix is much less than micrometer, which could possibly promote mechanical property of  $B_4C/Al$  composites as in situ nano-reinforcements.

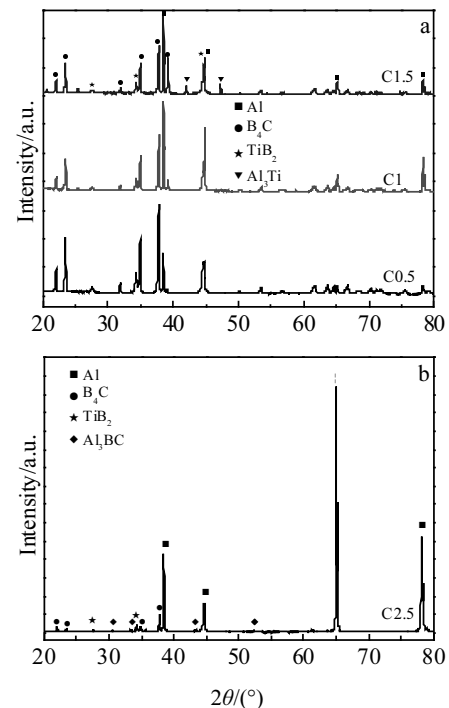


Fig.3 XRD patterns of  $B_4C/Al$  composites: (a) powder samples and (b) solid sample

Fig.5 presents the interfacial microstructure of  $B_4C/Al$  composites with various Ti contents and stirring time. When

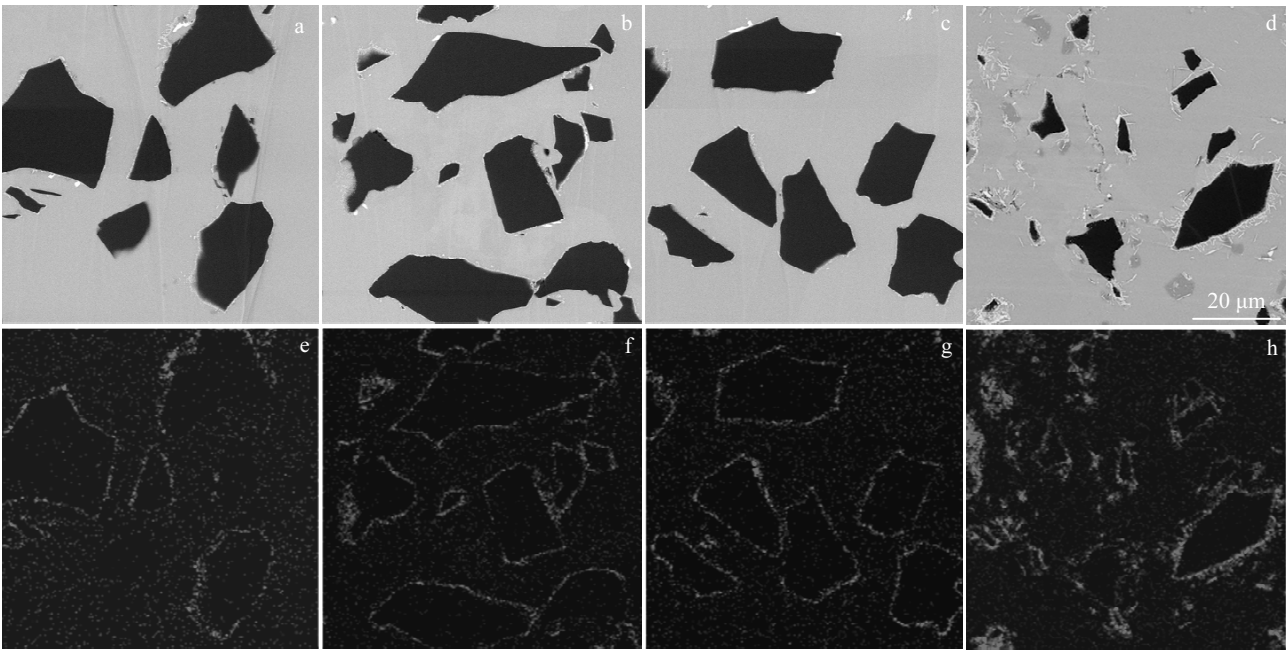


Fig.4 SEM images of B<sub>4</sub>C/Al composites: (a) C0.5, (b) C1, (c) C1.5, and (d) C2.5; corresponding distribution of Ti element recorded by EDS: (e) 0.5 wt%, (f) 1.0 wt%, (g) 1.5 wt%, and (h) 2.5 wt%

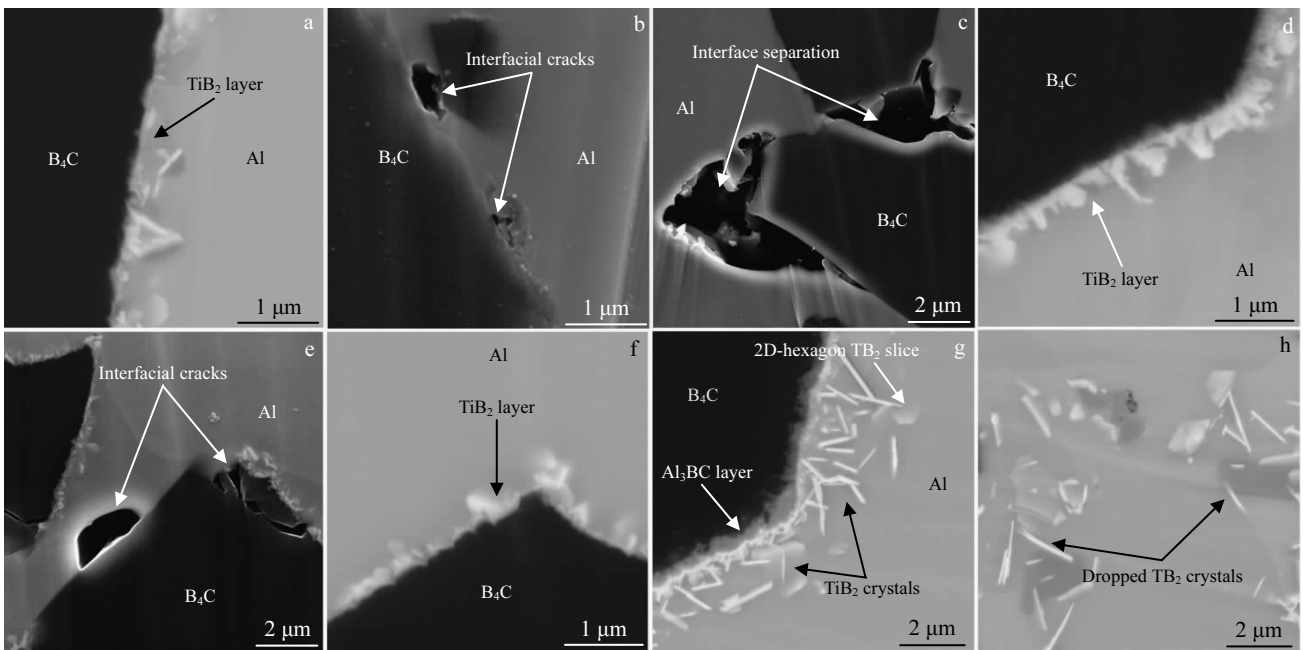


Fig.5 SEM images of interfacial microstructure in B<sub>4</sub>C/Al composites: (a~c) C0.5, (d, e) C1.0, (f) C1.5, and (g, h) C2.5

the addition of Ti element is 0.5 wt% (Fig.5a~5c), there are many defects like micro-holes and cracks at Al-B<sub>4</sub>C interface. Severe interface separation is even generated. However, intact TiB<sub>2</sub> layer still forms, which consists of fine grain layer and dispersive coarse TiB<sub>2</sub> crystals. When the addition of Ti element increases to 1 wt% (Fig.5d, 5e), the interface is

modified so that TiB<sub>2</sub> layer with more coarse TiB<sub>2</sub> crystals becomes continuous and compact. Although micro-defects occur, heavy interface separation is eliminated. Continuously increasing Ti content to 1.5 wt% (Fig.5f), intact interface reaction layer is obtained for all B<sub>4</sub>C particles. The gradual change of interface illustrates that Ti element in the melt

promotes interfacial microstructure modification and suppress the formation of defects. According to the evolution of interfacial microstructure, necessary Ti content for 15 wt% B<sub>4</sub>C/Al composites should be at least 1.5 wt%. Since B<sub>4</sub>C powders are integrally added into the melt at one time, aggregated B<sub>4</sub>C powders could not be immediately scattered, considering the limited dispersion ability of mechanical stirrer. Therefore, each B<sub>4</sub>C particle does not participate in the interfacial reaction at the same time, instead, in a successive way. Those B<sub>4</sub>C particles early contacting with liquid aluminum are more likely to generate intact TiB<sub>2</sub> layer through interfacial reaction. However, if B<sub>4</sub>C particles do not react with melt in time, they intend to obtain weak interface bonding with matrix because of poor wetting between B<sub>4</sub>C and liquid aluminum<sup>[21]</sup>. The number of covered B<sub>4</sub>C particles by TiB<sub>2</sub> depends on the Ti content in melt. Sufficient Ti element will ensure that all B<sub>4</sub>C particles are covered by a reaction layer finally. If Ti element is not enough, various interfacial microstructure like TiB<sub>2</sub> layer or interfacial defects will form. Further increasing Ti content and reaction time, interfacial microstructure will change to contain continuous TiB<sub>2</sub> layer and many detached TiB<sub>2</sub> particles because of severe interfacial reaction, as shown in Fig.5g and 5h. The former one is similar to the integral interface in other composites. However, many coarse TiB<sub>2</sub> crystals are detached from B<sub>4</sub>C surface and located near the interface or far into the aluminum matrix. It should be noted that a grey sublayer is formed between B<sub>4</sub>C and TiB<sub>2</sub> layer in Fig.5h. This sublayer is proved to be Al<sub>3</sub>BC in Fig.3b, which is a by-product through Eq.(2). During stirring process, the growth of TiB<sub>2</sub> crystals complies with nucleation and diffusion growth mechanism<sup>[15]</sup>. The size of TiB<sub>2</sub> nucleus becomes large along with stirring time. Due to strong shearing stress caused by flow field and growth mismatch stress, coarse TiB<sub>2</sub> crystals intend to deviate from growth site and to flow into the matrix. It is interesting that two kinds of TiB<sub>2</sub> crystal morphology are observed: slice and needle-like. The source Ti atoms of TiB<sub>2</sub> are generated by decomposition of Al<sub>3</sub>Ti compound in the melt. Due to sufficient Ti atoms, TiB<sub>2</sub> grow faster along with the matrix orientation than along with other directions. TiB<sub>2</sub> with hexagon crystal structure prefers to grow into 2D-hexagon slice, as shown in Fig.5g. In fact, both morphologies are different section of hexagon TiB<sub>2</sub> crystal. It is promising that these nanoscale second precipitations TiB<sub>2</sub> will further strengthen the matrix and influence mechanical property of B<sub>4</sub>C/Al composites<sup>[22]</sup>.

## 2.2 Mechanical property

Typical tensile curves of B<sub>4</sub>C/Al composites are shown in Fig.6 and the tensile properties are summarized in Table 2. It is clear that the interfacial reaction has an effect on the tensile properties. Both average yield strength (0.2%) and ultimate tensile strength basically become large with enhanced Ti content, 46.4 and 93.2 MPa for C0.5, however, 85.4 and 138.9 MPa for C2.5. Increased strengths illustrate that interfacial

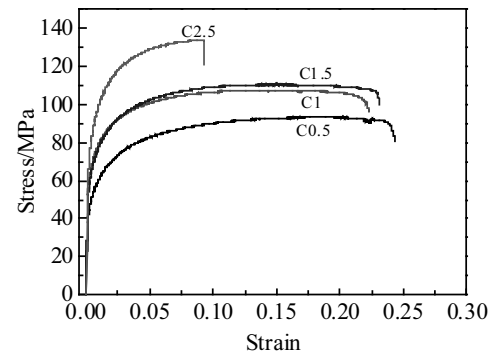


Fig.6 Typical tensile curves of B<sub>4</sub>C/Al composites with different Ti contents

Table 2 Tensile properties of B<sub>4</sub>C/Al composites

Composites	C0.5	C1	C1.5	C2.5
$\sigma_{0.2\%}$ /MPa	46.4±0.3	69.4±6.4	60.6±0.5	85.4±6.6
$\sigma_b$ /MPa	93.2±1.0	110.6±1.8	111.1±0.5	138.9±6.2
$\delta$ /%	27.1±1.6	19.8±2.1	19.1±2.8	6.9±1.5

$\sigma_{0.2\%}$ : yield strength at 0.2% strain;  $\sigma_b$ : ultimate tensile strength;  $\delta$ : ductility

reaction promotes the composite strengthening. The low yield stress of C0.5 indicates that defects generally exist in the matrix, which is in accord with the microstructure shown in Fig.5b, 5c. But the deformation ability is compromised, especially for C2.5 with an average ductility of 6.9%. SEM pictures of fracture surface at low magnification are presented in Fig.7. Many toughening dimples with knife edges and the wavy appearance of the serpentine glide on the dimple walls are observed on the fracture surfaces of all B<sub>4</sub>C/Al composites, which illustrates that a void growth and coalescence mechanism by shearing stress dominates during fracture process. The dimples are essentially equiaxial and nearly uniform in size. However, the dimple size is much different that dimples gradually become small with increasing Ti content. Many fine dimples presented in Fig.7d indicate insufficient evolution of plastic deformation, which is consistent with the low ductility exhibited by C2.5.

Fig.8 shows interfacial fracture morphologies of B<sub>4</sub>C/Al composites after tensile test. For C0.5, there are basically two kinds of interfacial microstructures existing in the matrix, well-bonded interface and interfacial defects, such as cracks, holes and interfacial decohesion. Well-bonded interface is generated because of addition Ti. However, considering the shortage of active Ti element, it is difficult for all particle surface to be covered by continuous and compact TiB<sub>2</sub> layer. Due to the poor wetting between B<sub>4</sub>C and Al melt<sup>[21,23]</sup>, various interface defects form during solidification process. These defects indicate that weak interface combination universally exists in C0.5. Due to the weak physical bonding between B<sub>4</sub>C

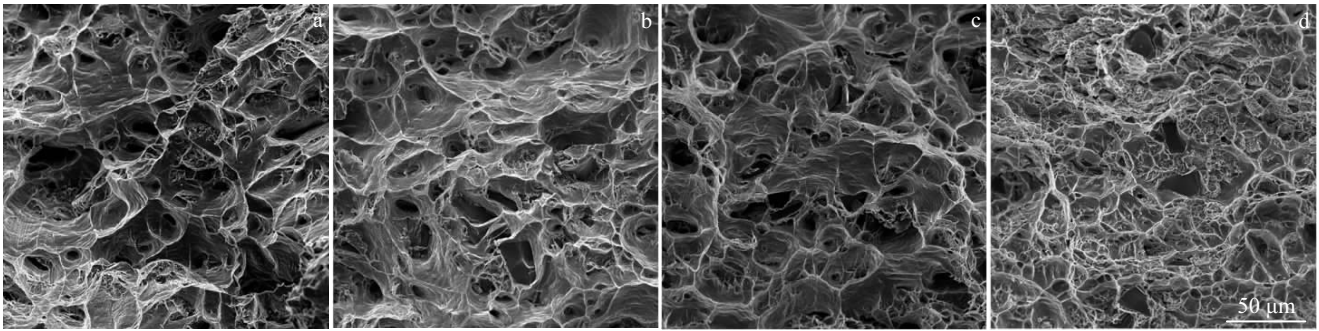


Fig.7 SEM fracture surface morphologies of  $B_4C/Al$  composites: (a) C0.5, (b) C1, (c) C1.5, and (d) C2.5

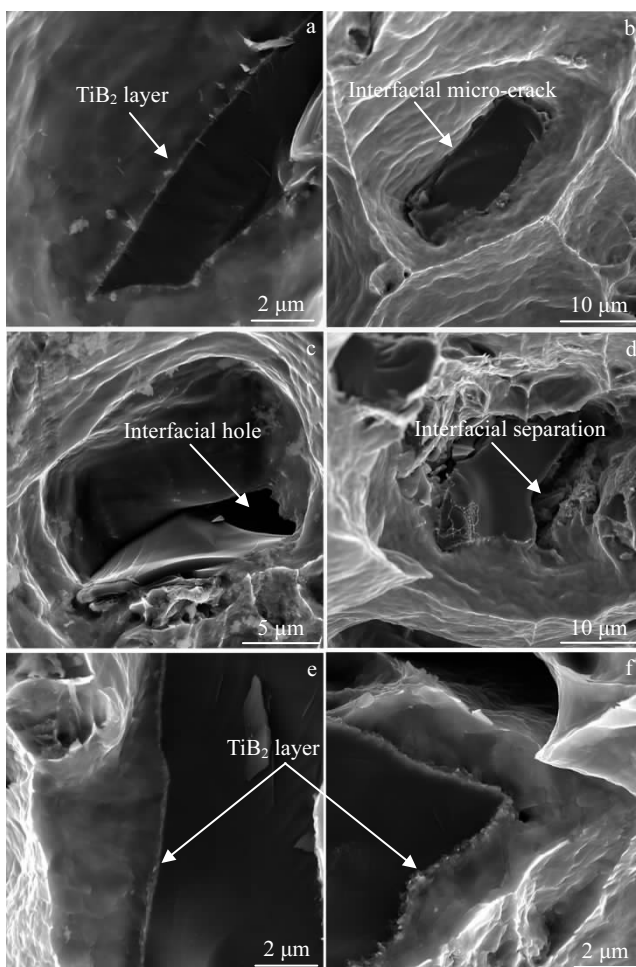


Fig.8 SEM images of interfacial fracture microstructures for  $B_4C/Al$  composites after tensile test: (a~d) C0.5, (e) C1, and (f) C1.5

particles and matrix, interface is the easier sites for crack generation and diffusion. Crack propagation predominantly occurs by decohesion at the particle-matrix interface. Some  $B_4C$  reinforcements with sharp edges (Fig.8c, 8d), which are features of original  $B_4C$  particles in as-received condition, indicate that they do not share load during tensile process.

With the increasing of Ti content, different interfacial fracture behavior is observed in C1 and C1.5, as shown in Fig.8e, 8f.  $B_4C$  particles with flat and smooth surface are located on the fracture surface, which proves that particles have been broken up during the tensile process. Ruptured hard particles indicate that effective load transfer happens through the interface and is a proof of strong particle-matrix bonding<sup>[5,10]</sup>. Continuous  $TiB_2$  layer exists at the interface, acting as a transition zone between  $B_4C$  particles and aluminum matrix. Since the wetting angles ( $90^\circ$ ) between Al melt and  $TiB_2$  is much lower than that ( $127^\circ$ ) between Al melt and  $B_4C$ <sup>[21,24]</sup>, improved wetting property helps to eliminate interfacial defects and form tight chemical interface combination. Therefore, load transfer through  $TiB_2$  layer could take place during the tensile test. Hard  $B_4C$  particles act as reinforcements to strengthen the matrix and the mechanical property of  $B_4C/Al$  composites is enhanced.

The interfacial fracture surface of C2.5 is shown in Fig.9. Due to sufficient interface reaction, continuous  $TiB_2$  layer is similarly generated at  $B_4C-Al$  interface in C2.5. Fracture surface presents broken  $B_4C$  particles, which illustrates that load transfer occurs through  $TiB_2$  layer. A noteworthy morphology in Fig.9a is the fine dimples near Al- $B_4C$  interface, which are not produced on fracture surface of other  $B_4C/Al$  composites. Although the largest strength is achieved for C2.5, its ductility decreases to a lower level, about 6.9%. This change could be explained by the fine dimples. From the EDS map in Fig.9b, Ti element clearly concentrates at the core of fine dimples. Considering the nanoscale  $TiB_2$  crystals, shown in Fig.5h, the Ti enrichment is aroused by departed  $TiB_2$  crystals. Fig.9c presents a higher magnification image of fine dimples. Some slice-like  $TiB_2$  crystals are located at the center of fine dimples. These  $TiB_2$  particles occupy dimple center, resulting in the formation of many fine dimples. Small dimple size leads to limited deformation of aluminium matrix and thus lower ductility. However, the formation of nanoscale  $TiB_2$  particles introduces many in situ second reinforcements into the matrix of C2.5. Due to the nanoscale size and higher wettability with Al than  $B_4C$  particles,  $TiB_2$  crystals effectively

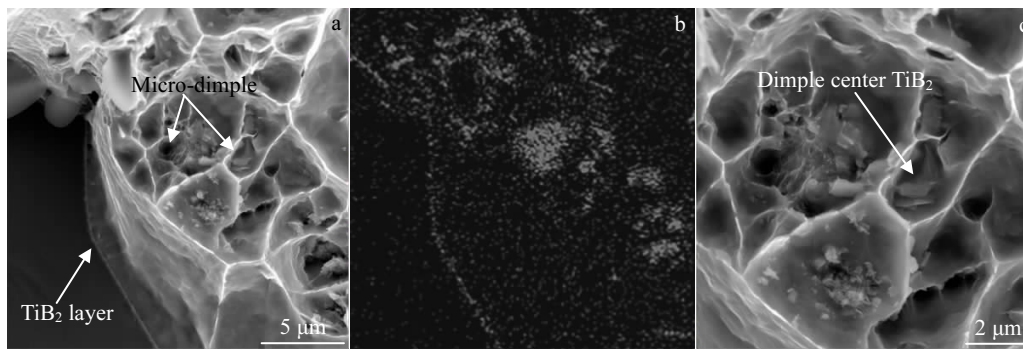


Fig.9 Interfacial fracture microstructures of C2.5 after tensile test: (a) reaction layer TiB<sub>2</sub> and fine dimples, (b) EDS map of Ti element corresponding Fig.9a, and (c) higher magnification image of the fine dimples

strengthen the matrix and increase tensile strength of B<sub>4</sub>C/Al composites.

Considering normalized matrix of four B<sub>4</sub>C/Al composites, the results listed above illustrate that the mechanical property of B<sub>4</sub>C/Al composite can be improved by transition element Ti through interfacial reaction. In metal matrix composites, the contribution of reinforcements to mechanical property strongly depends on how closely the matrix and reinforcements combine<sup>[7]</sup>. Well bonded interface helps to effectively transfer loads to hard particles, improving the strength of composite materials. On the contrary, if weakly bonded interface or interfacial defects are formed, loads transfer will be impacted and the strength effect of reinforcement is limited<sup>[5]</sup>. In this experiment, the strength gradually increases along with enhanced interfacial reaction, which is related to the formation of TiB<sub>2</sub> nanolayer. Interfacial reaction makes a chemical bonding between B<sub>4</sub>C particles and Al matrix, which is firmer compared with mechanical occlusion of physics surface. This TiB<sub>2</sub> layer results in modification of interface microstructure and eliminates interfacial defects because of improved wetting property with Al melt. For the chemically bonded interface, a crystallographic orientation relationship is likely to exist on both sides of the interface<sup>[10]</sup>. TiB<sub>2</sub> layer makes B<sub>4</sub>C closely combine with the Al matrix, and promotes effective load transfer.

The interfacial TiB<sub>2</sub> layer also changes the fracture behavior of B<sub>4</sub>C/Al composites. The fracture morphology presented in Fig.8 and 9 displays a clear difference between B<sub>4</sub>C particles coated with and without TiB<sub>2</sub> layer. The former one mainly fails in the form of reinforcement breakage; however, the later one, with interfacial defects, fails in the form of interface departure, and B<sub>4</sub>C particles are unbroken. The mechanism of two kinds of fracture behaviors is essentially a competitive relation between interface strength and reinforcement strength. If the strength of interface is greater than that of reinforcement, fracture will give priority to particle breakage; if the strength of interface is lower than that of reinforcement, interface

failure is easier to happen. Different failure modes presented above indicate that TiB<sub>2</sub> layer strongly improves interfacial bonding strength in a way of B<sub>4</sub>C particles breakage.

### 3 Conclusions

1) The addition of Ti element into the melt helps to form TiB<sub>2</sub> chemical-bonding interface through interfacial reaction. When the content of Ti is over much, which is about 1.5 wt% for 15 wt% B<sub>4</sub>C particles, the surfaces of B<sub>4</sub>C are covered by fine, continuous and dense TiB<sub>2</sub> layer. Thus B<sub>4</sub>C-Al interface obtains strong bonding. However, when Ti content is insufficient, lots of interfacial defects are unavoidably formed.

2) The interfacial modification on B<sub>4</sub>C through regulating the interfacial microstructure has an influence on mechanical property of B<sub>4</sub>C/Al composites. As the degree of interfacial reaction increases, B<sub>4</sub>C/Al composites with finer TiB<sub>2</sub> layer present higher tensile strength, but the elongation decreases.

3) Fracture behavior of B<sub>4</sub>C/Al composites is given priority to a void coalescence mechanism. TiB<sub>2</sub> layer eliminates the interfacial defects, makes an effective load transfer process, and improves the strength by breakage of B<sub>4</sub>C particles. The coarse TiB<sub>2</sub> crystals generated by interfacial reaction further strengthen the matrix as in situ second reinforcements, but also result in smaller toughening dimples and thus lower ductility.

### References

- 1 Zheng J, Shu G, Wang W et al. *Applied Surface Science*[J], 2015, 349: 733
- 2 Bonnet G, Rohr V, Chen X G et al. *Packaging, Transport, Storage & Security of Radioactive Material*[J], 2009, 20(3): 98
- 3 Zhang P, Li Y, Wang W et al. *Journal of Nuclear Materials*[J], 2013, 437(1-3): 350
- 4 Lai J, Zhang Z, Chen X G. *Journal of Alloys and Compounds*[J], 2013, 552: 227
- 5 Song J, Guo Q, Ouyang Q et al. *Materials Science and Engineering A*[J], 2015, 644: 79
- 6 Guo X, Guo Q, Li Z et al. *Scripta Materialia*[J], 2016, 114: 56

- 7 Chawla N, Shen Y L. *Advanced Engineering Materials*[J], 2001, 3(6): 357
- 8 Zhang H, Ramesh K, Chin E. *Acta Materialia*[J], 2005, 53(17): 4687
- 9 Zhang H, Chen M W, Ramesh K T et al. *Materials Science and Engineering A*[J], 2006, 433(1-2): 70
- 10 Tham L M, Gupta M, Cheng L. *Acta Materialia*[J], 2001, 49(16): 3243
- 11 Tham L M, Gupta M, Cheng L. *Materials Science and Engineering A*[J], 2003, 354(1-2): 369
- 12 Li Y, Li Q, Liu W et al. *Journal of Alloys & Compounds*[J], 2016, 684: 496
- 13 Zhang Z, Chen X G, Charette A. *Journal of Materials Science*[J], 2007, 42(17): 7354
- 14 Viala J C, Bouix J, Gonzalez G et al. *Journal of Materials Science*[J], 1997, 32(17): 4559
- 15 Zheng J, Li Q, Liu W et al. *Journal of Composite Materials*[J], 2016, 50: 3843
- 16 Zhang Z, Fortin K, Charette A et al. *Journal of Materials Science*[J], 2011, 46(9): 3176
- 17 Kennedy A R, Brampton B. *Scripta Materialia*[J], 2001, 44(7): 1077
- 18 Kennedy A R. *Journal of Materials Science*[J], 2002, 37(2): 317
- 19 Jiang L, Wen H, Yang H et al. *Acta Materialia*[J], 2015, 89: 327
- 20 Luo Z, Song Y, Zhang S et al. *Metallurgical and Materials Transactions A*[J], 2012, 43(1): 281
- 21 Kocafe D, Sarkar A, Chen X. *International Journal of Materials Research*[J], 2012, 103(6): 729
- 22 Lü L, Lai M O, Su Y et al. *Scripta Materialia*[J], 2001, 45(9): 1017
- 23 Wang Z, Li Q, Zheng J et al. *Rare Metal Materials & Engineering*[J], 2017, 46(9): 2345
- 24 Lin Q, Shen P, Qiu F et al. *Scripta Materialia*[J], 2009, 60(11): 960

## Ti 元素对 B<sub>4</sub>C/Al 复合材料力学性能的改善作用

阮 晴<sup>1</sup>, 贾玉振<sup>2</sup>, 郑继云<sup>2</sup>, 李丘林<sup>3</sup>, 刘 伟<sup>1</sup>, 束国刚<sup>4</sup>

(1. 清华大学, 北京 100084)

(2. 中国核动力研究设计院 反应堆燃料及材料重点实验室, 四川 成都 610041)

(3. 清华大学深圳研究生院, 广东 深圳 518055)

(4. 中广核工程有限公司, 广东 深圳 518055)

**摘 要:** 良好的结合界面对金属基复合材料的性能至关重要。利用液态搅拌法, 制备了一种 B<sub>4</sub>C 强化的 B<sub>4</sub>C/Al 复合材料。通过添加 Ti 元素, 探讨了界面对材料的界面结构和力学性能的影响。研究发现, 通过 B<sub>4</sub>C 和 Al 熔体之间的界面反应, Ti 元素大量聚集于 B<sub>4</sub>C/Al 界面处。B<sub>4</sub>C 颗粒表面形成了一层致密且连续的纳米 TiB<sub>2</sub> 界面层, 实现了界面改性。由于 TiB<sub>2</sub> 界面层具有良好的润湿性和结合状态, B<sub>4</sub>C/Al 原有的界面缺陷消除了。随着界面反应程度的加强, 材料强度逐渐提高。剧烈的界面反应会形成大量脱落的纳米 TiB<sub>2</sub> 颗粒进入基体。纳米 TiB<sub>2</sub> 颗粒作为原位第二强化相进一步增强基体。最后, 探讨了不同程度界面改性后 B<sub>4</sub>C/Al 复合材料的断裂行为。

**关键词:** B<sub>4</sub>C/Al 复合材料; 钛; 界面反应; 力学性能

作者简介: 阮 晴, 女, 1993 年生, 硕士, 清华大学材料学院, 北京 100084, 电话: 010-62772852, E-mail: rq15@mails.tsinghua.edu.cn